Effect of the Branch Length on Structural and Separation Properties of Hyperbranched Poly(1,3-dioxolane)

Liang Huang,[1] Wenji Guo,[1] Himangshu Mondal,[1] Skye Schaefer,[1] Thien N. Tran,[1] Shouhong Fan,[2] Yifu Ding,[2] and Haiqing Lin[1]*

[1]Department of Chemical and Biological Engineering, University at Buffalo, The State University of New York, Buffalo, NY 14260, USA

[2]Membrane Science, Engineering and Technology (MAST) Center, Paul M. Rady Mechanical Engineering, University of Colorado at Boulder, Boulder, CO 80309, USA

* Corresponding author: haiqingL@buffalo.edu (H. Lin)

Prepared for submission to *Macromolecules*

For Table of Contents Use Only

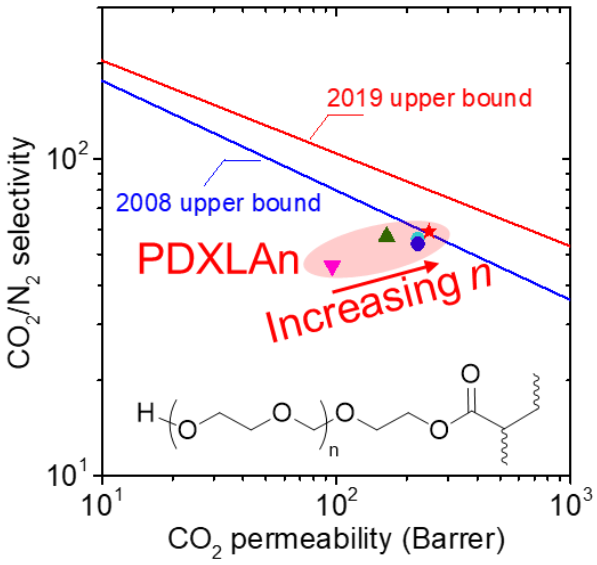

ABSTRACT

Polymers containing poly(ethylene oxide) (PEO) demonstrate superior membrane CO_2/N_2 separation properties owing to their polar ether oxygen groups exhibiting strong affinity towards CO_2. Poly(1,3-dioxolane) (PDXL) shows ether oxygen content higher than PEO and is expected to have higher CO_2/N_2 solubility selectivity. However, similar to PEO, the high crystallinity of PDXL greatly reduces its gas permeability. Herein, amorphous PDXL-based hyperbranched polymers were synthesized by ring-opening of 1,3-dioxolane (DXL) to form poly(1,3-dioxolane) acrylate (DXLAn) followed by photopolymerization. The repeating unit of DXL (*n*) or branch length was systematically varied from 4 to 12 to yield amorphous polymers. The chemical and physical properties of the obtained polymers (PDXLAn) were thoroughly evaluated and used to interpret pure- and mixed-gas transport characteristics. The polymers exhibit attractive CO_2/N_2 and CO_2/CH_4 separation properties. For example, PDXLA8 exhibits CO_2 permeability of 220 Barrer and CO_2/N_2 selectivity of 56 at 35 ℃, surpassing Robeson's 2008 upper bound, and it shows robust separation performance when evaluated with simulated flue gas at 60 ℃. This study demonstrates that hyperbranched structures are an effective route to construct amorphous yet highly polar polymers and that chain end groups are instrumental in determining structural and gas transport characteristics.

KEYWORDS: poly(1,3 dioxolane), membranes, carbon capture, hyperbranched polymers, CO_2/N_2 separation

■ INTRODUCTION

The use of fossil fuels produces vast amounts of flue gas, which mainly consists of CO_2 and N_2, and has become one of the most significant contributors to CO_2 emissions. One important strategy to reduce CO_2 emissions is to capture CO_2 from the post-combustion flue gas. Polymeric membranes have emerged as one of the leading technologies for CO_2 capture due to their high energy efficiency, facile scalability, operation and maintenance, and small footprint.[1-3] As the flue gas has a huge volume and low CO_2 partial pressure, membrane materials should exhibit both high CO_2 permeability and CO_2/N_2 selectivity to minimize the size of the membrane skid and maximize the purity of the product.[3]

Various polymeric materials have been designed and engineered for high-performance CO_2/N_2 separation, such as thermally rearranged (TR) polymers,[4-6] polymers of intrinsic microporosity (PIMs),[7, 8] polyamines,[9, 10] polyimides,[11] and mixed-matrix materials (MMMs).[9, 12] In particular, polymers containing poly(ethylene oxide) (PEO) have emerged as leading materials for this application because of their affinity towards CO_2 (resulting in superior CO_2/gas solubility selectivity) and flexible polymer chains (leading to high CO_2 diffusivity).[13-16] For example, block copolymers (*e.g.*, Pebax® and PolyActive™),[17-22] cross-linked PEO,[15, 23-26] and MMMs[27-30] have been demonstrated with an excellent combination of high CO_2 permeability and CO_2/N_2 selectivity.

Further increase of ether oxygen contents in polymers is expected to improve CO_2/N_2 solubility selectivity and thus permeability selectivity. Recently, we have synthesized polymers based on 1,3-dioxolane (DXL with an O/C molar ratio of 0.67), which has ether oxygen content higher than PEO (O/C ratio: 0.5).[31, 32] As high molecular weight polymers based on DXL tend to crystallize (reducing gas permeability), hyperbranched polymers (PDXLAn) with short branches

of DXL were synthesized from poly(1,3-dioxolane) acrylate (DXLAn with n = 12). The short branches suppress crystallization while achieving high content of ether oxygens (40 mass%).[25, 32] For example, PDXLA12 was amorphous and had glass transition temperature (T_g) of –66 °C, and it displayed CO_2 permeability of 200 Barrer (1 Barrer = 10^{-10} cm^3(STP) cm cm^{-2} s^{-1} $cmHg^{-1}$) and CO_2/N_2 selectivity of 60 at 35 °C. Such performance is better than its PEO analog prepared from poly(ethylene glycol) acrylate (PEGA with n = 7), which showed CO_2 permeability of 120 Barrer and CO_2/N_2 selectivity of 46 at 35 °C.[25] However, there lacks a systematic study of the impact of the n values on physical and gas transport properties of the polymers, which is critical to understand the structure/property relationship and guide the design of high-performance membranes for CO_2/N_2 separations.

Herein we present an improved method to synthesize a systematic series of DXLAn with a well-controlled DXL chain length (n) ranging from 4 to 20, which were then photopolymerized to form hyperbranched PDXLAn films. The structural and gas transport characteristics of PDXLAn are thoroughly investigated to derive the relationship between structure and CO_2/gas separation properties. Pure- and mixed-gas CO_2/N_2 separation properties were thoroughly evaluated. PDXLA8 displays the best combination properties with CO_2 permeability of 220 Barrer and CO_2/N_2 selectivity of 56 at 35 °C, surpassing Robeson's 2008 upper bound. When challenged with model flue gas containing 20% CO_2 and 80% N_2, PDXLA8 shows robust CO_2/N_2 separation performance at temperatures up to 60 °C. Additionally, PDXLA8 exhibits good CO_2/CH_4 separation performance at 35 and 50 °C, making it appealing for practical natural gas processing.

■ RESULTS AND DISCUSSION

Synthesis and characterization of the DXLAn and PDXLAn. Figure 1a displays the synthesis of the macromonomers of DXLAn from 1,3-dioxolane (DXL) using cationic ring-opening polymerization with triflic acid (TfOH) as the initiator and 2-hydroxyethyl acrylate (HEA) as the chain transfer reagent.[31, 32] The TfOH:HEA molar ratio increases from 1:16 in the previous method to 1:9 in this work, which reduces the reaction time from 12 to 3 h while achieving a similar yield of DXLn and better control of the DXL chain length. Figure 1b shows the ^{1}H NMR spectrum of DXLA8 and the assignment of the chemical shifts for the protons. The protons (g and f) in the DXL unit have chemical shifts of 3.73 and 4.76 ppm, and α-acryloyl protons (a, b, and c) have chemical shifts of 5.82, 6.13, and 6.42 ppm. The *n* values are calculated by comparing the intensities of g and f with those of a, b, and c. In this study, five DXLAn macromonomers were synthesized with actual *n* values of 3.6, 6.5, 8.3, 9.8, and 11.9, and they are named DXLA4, DXLA6, DXLA8, DXLA10, and DXLA12, respectively. The NMR spectra of DXLA4, DXLA6, DXLA10, and DXLA12 are presented in Figure S1. The calculated *n* values are very similar to the theoretical values (*i.e.*, the molar ratio of DXL to HEA).[32-34] The molecular weight and polydispersity of the DXLA8 were also analyzed using electrospray ionization (ESI)-mass spectroscopy (MS). The Mn of DXLA8 is 797 g/mol (Figure S2), which is close to that (731 g/mol) measured by NMR. Additionally, the DXLA8 shows the Mw of 836 g/mol and thus PDI of 1.05, indicating the narrow molecular weight distribution of DXLA8 and good control of chain length using our improved method.

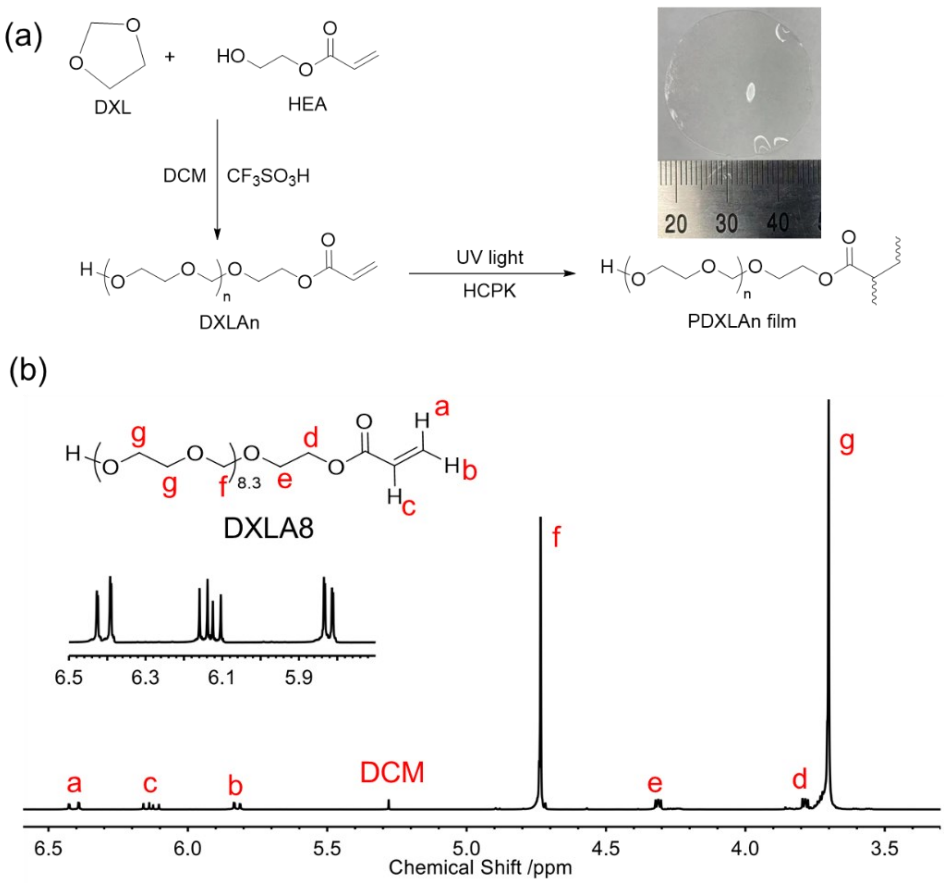

Figure 1. (a) Synthetic route of the macromonomers of DXLAn and the corresponding PDXLAn films. The inset is the photo of a PDXLA8 film (diameter: ~2.5 cm). (b) ^{1}H NMR spectrum of DXLA8.

DXLAn ($n \leq 12$) were then photopolymerized using 1-hydroxycyclohexyl phenyl ketone (HCPK) as an initiator to prepare PDXLAn films (Figure 1a). Because of its high molecular weight (998 g/mol), DXLA12 is a viscous liquid at ≈ 23 °C and needs precaution to avoid any bubbles when preparing the PDXLA12 films, and therefore, only PDXLAn ($n \leq 12$) films were prepared and tested for gas transport properties. As shown in the FTIR spectra (Figure S3), the absorption peaks of double bonds in DXLA8 almost disappear after the photopolymerization, indicating the near-complete conversion of the acrylate groups. The PDXLAn films cannot be dissolved in

typical solvents (e.g., water, methanol, and dimethylformamide), indicating the occurrence of cross-linking. Similar phenomena have been noted for the polymers derived from PEGA[25] and DXLA12,[32] and the cross-linking can be ascribed to the trace amount of diacrylates produced during the macromonomer synthesis or chain transfer during the photopolymerization. As such, PDXLAn cannot be directly used to prepare coating solutions to manufacture thin-film composite (TFC) membranes, and a controlled polymerization method should be developed to prepare high molecular weight, soluble polymers, which is beyond the scope of this study.

Figure 2a shows differential scanning calorimetry (DSC) thermograms for PDXLAn. There are no crystallization or melting peaks, suggesting that the PDXLAn are completely amorphous. The X-ray diffraction (XRD) patterns of the PDXLAn films also confirm their amorphous structure at ≈ 23 °C (Figure S4a). These results demonstrate that the approach of short branches successfully prohibits the crystallization of polar ether groups.

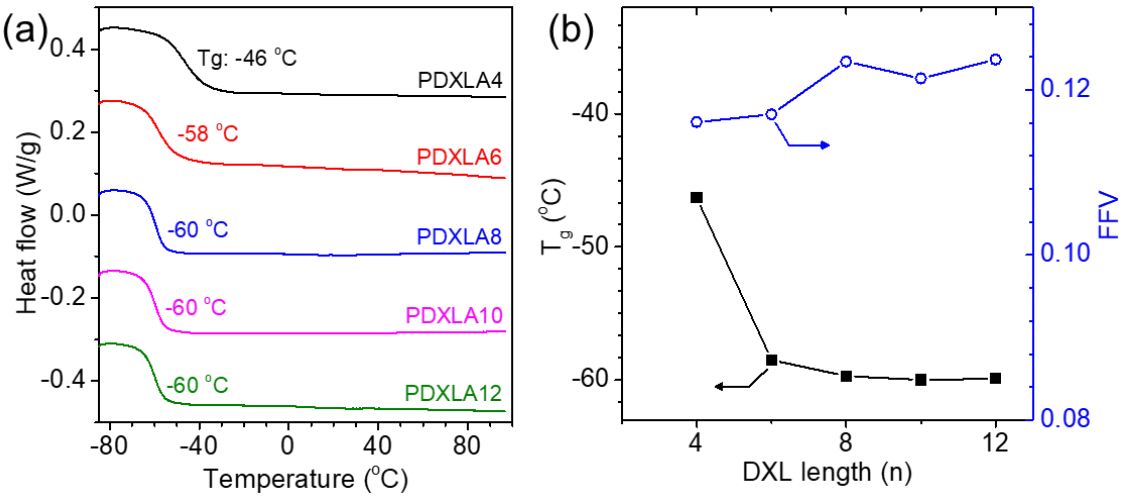

Figure 2. (a) DSC curves of PDXLAn films. (b) Effect of the DXL chain length (n) on the *FFV* and T_g of the PDXLAn films.

Figure 2b shows that the T_g of PDXLAn decreases with increasing DXL branch length before leveling off. For example, the T_g decreases from –46 ℃ for PDXLA4 to –60 ℃ for PDXLA8, PDXLA10, and PDXLA12, which can be ascribed to the change of the content of the hydroxyl (-OH) groups in the PDXLAn. The -OH groups can form hydrogen bonding with the oxygen atom, reducing the polymer chain flexibility and increasing the T_g.[25, 35, 36] As shown in Table S1 and Figure S4b, PDXLA4 has an -OH content of 4.4 mass%, almost double that of PDXLA8 (2.3 wt%), and further increase of the chain length from 8 to 12 only decreases the -OH content to 1.7 mass%. Consequently, PDXLA8, PDXLA10, and PDXLA12 show similar T_g values. The PDXLAn samples are also compared with a PEO analog prepared from poly(ethylene glycol) acrylate (PEGAn with n = 7 and Mn = 380 g/mol). As shown in Table S1, PEGA7 shows a T_g of -40 ℃ because of its high -OH content (4.5 mass%). The mechanical properties of the PDXLAn films were also tested (Figure S5). Increasing the chain length reduces the tensile strength and Young's modulus and improves the elongation at break, which can also be ascribed to the decreased -OH content and thus hydrogen bonding. As such, PDXLA4 with the higher -OH content shows greater tensile strength and Young's modulus and lower elongation at break than PDXLA8 and PDXLA12.

The density (ρ_p) of the PDXLAn films decreases with increasing the n values due to the decreased -OH content. The fractional free volume (FFV) is often estimated using the following equation:

$$FFV = 1 - 1.3\rho_p V_W \quad (1)$$

where V_W is the van der Waals volume estimated using the group contribution method. Figure 2b presents that the FFV of PDXLAn increases with increasing n values, consistent with the decreased -OH content.

Effect of the branch length on pure-gas transport properties of PDXLAn. Figure 3a displays that the pure-gas permeability of PDXLAn at 35 ℃ follows an order of $CO_2 > H_2 > C_2H_6 > CH_4 > N_2$, similar to the PEO-based polymers.[14, 25] Increasing the *n* value increases the gas permeability before leveling off at the *n* value greater than 8. For example, CO_2 permeability increases from 96 Barrer for PDXLA4 to 220 Barrer for PDXLA8 and 250 Barrer for PDXLA12 because PDXLA8 and PDXLA12 have lower T_g and higher *FFV* than PDXLA4. Figure 3b depicts the effect of the DXL chain length on CO_2/gas selectivity. As the *n* value increases from 4 to 6, the CO_2/N_2 selectivity significantly increases from 46 to 57, and it becomes almost stable after n ≥ 6. The CO_2/H_2 selectivity slightly increases while CO_2/C_2H_6 selectivity gradually decreases with increasing *n* values (Figure 3b). The chain length does not have a significant impact on the CO_2/CH_4 selectivity (ranging from 18 to 22), given its uncertainty of ≈ 10%. By contrast, PDXLA8 shows CO_2 permeability (220 Barrer) and CO_2/CH_4 selectivity (22) higher than PEGA7 (with CO_2 permeability of 120 Barrer and CO_2/CH_4 selectivity of 16), demonstrating the advantage of the DXL-based polymers over PEO-based polymers.

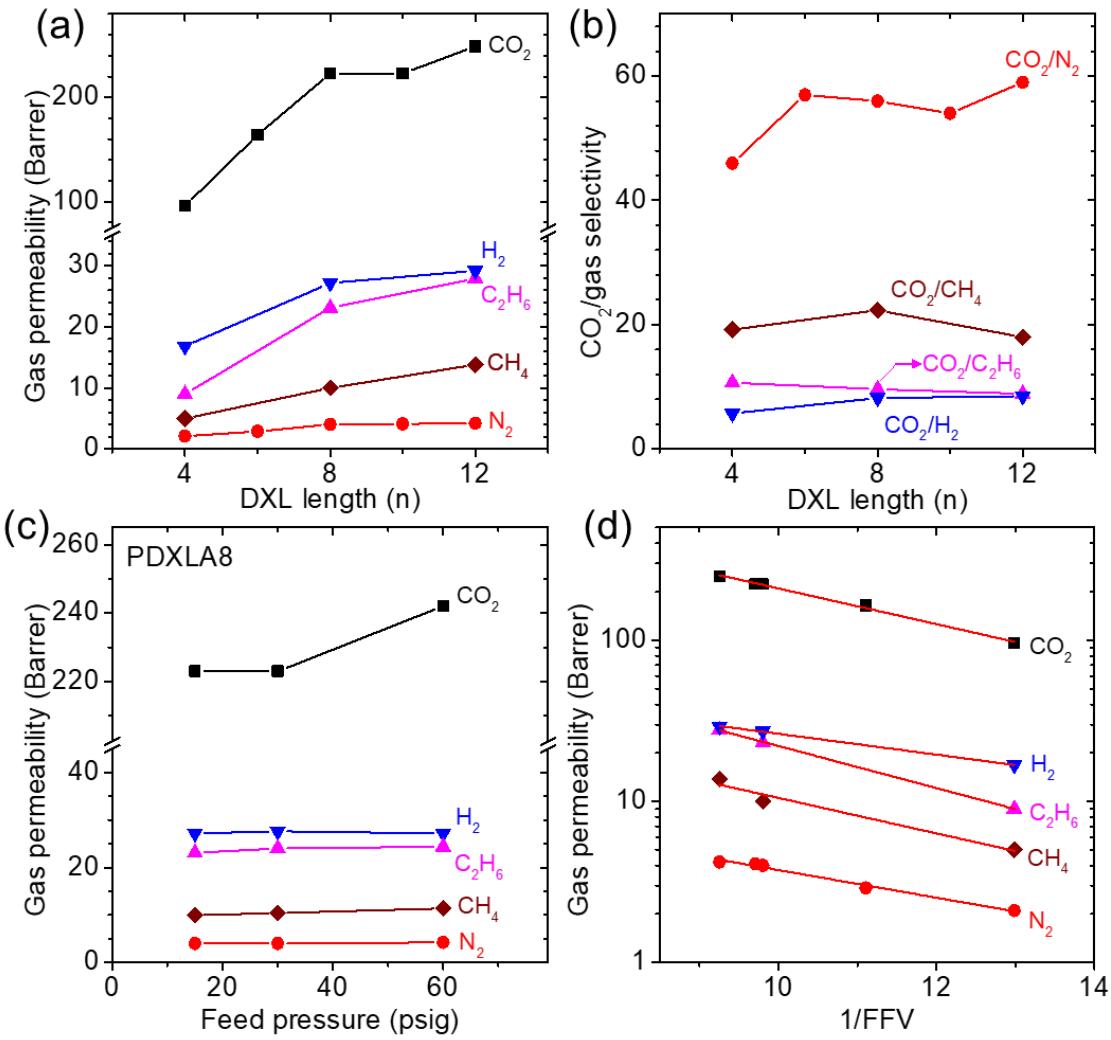

Figure 3. Effect of the DXL chain length (*n*) on (a) the pure-gas permeability and (b) CO_2/gas selectivity at 35 °C and 2.0 bar. (c) Pure-gas permeability of PDXLA8 at different feed pressures. (d) Modeling of gas permeability using the free volume model (*i.e.*, Equation 2).

Figure 3c presents the effect of the feed pressure on the pure-gas permeability of PDXLA8 at 35 °C. CO_2 permeability increases from 220 Barrer at 2.0 bar to 240 Barrer at 5.1 bar because of the high CO_2 sorption and thus plasticization of polymer chains, increasing the polymer chain flexibility and gas diffusivity.[37, 38] On the other hand, the permeability of other gases (H_2, N_2, CH_4, and C_2H_6) is independent of the feed pressure because of their low sorption in the polymer.[38]

Gas diffusivity depends sensitively on the *FFV* of the polymer. If the polymer compositions have negligible impact on the gas solubility, gas permeability can be expressed using Equation 2:[37]

$$P = A\ exp\left(-\frac{B}{FFV}\right) \quad (2)$$

where A is a front factor (Barrer), and B is a parameter increasing with the increasing kinetic diameter of the penetrants. Figure 3d exhibits that the permeabilities of all tested gases can be satisfactorily modeled using Equation 2. The constant B is 0.15 for H_2 (with the kinetic diameter of 2.89 Å), 0.26 for CO_2 (3.3 Å), 0.20 for N_2 (3.64 Å), 0.25 for CH_4 (3.8 Å), and 0.30 for C_2H_6 (4.44 Å), which follows the same increasing order of their kinetic diameter except for CO_2.

To thoroughly elucidate the effect of the DXL chain length on gas transport properties, CO_2 and C_2H_6 sorption isotherms of PDXLAn were determined at 35 °C, and the results are displayed in Figures 4a,b and S4. N_2 sorption is below the detection limit of our apparatus, and therefore, C_2H_6 is used as a marker for gas molecules without specific interactions with PDXLAn.[32] For all PDXLAn films, the CO_2 and C_2H_6 sorption increase linearly with the pressure, and the sorption isotherms can be described by Henry's law because of their rubbery nature.[25, 39] As presented in Figure 3c and Table S2, CO_2 (with a critical temperature of 304 K) exhibits higher solubility than C_2H_6 (305 K) despite their similar critical temperature, confirming the affinity of PDXLAn with CO_2. Figure 4c shows that increasing the n value decreases C_2H_6 solubility due to the decreased *FFV* but has a negligible effect on CO_2 solubility caused by the opposite effect of decreased *FFV* and increased ether oxygen content (Table S1). As such, the CO_2/C_2H_6 solubility selectivity slightly decreases with the increase of DXL chain length. The PDXLAn demonstrates CO_2/C_2H_6 solubility selectivity higher than PEGA7 and PEGDA-*co*-PEGMEA (≈2.5),[25, 40] further confirming that higher ether oxygen content leads to higher CO_2/gas solubility selectivity.

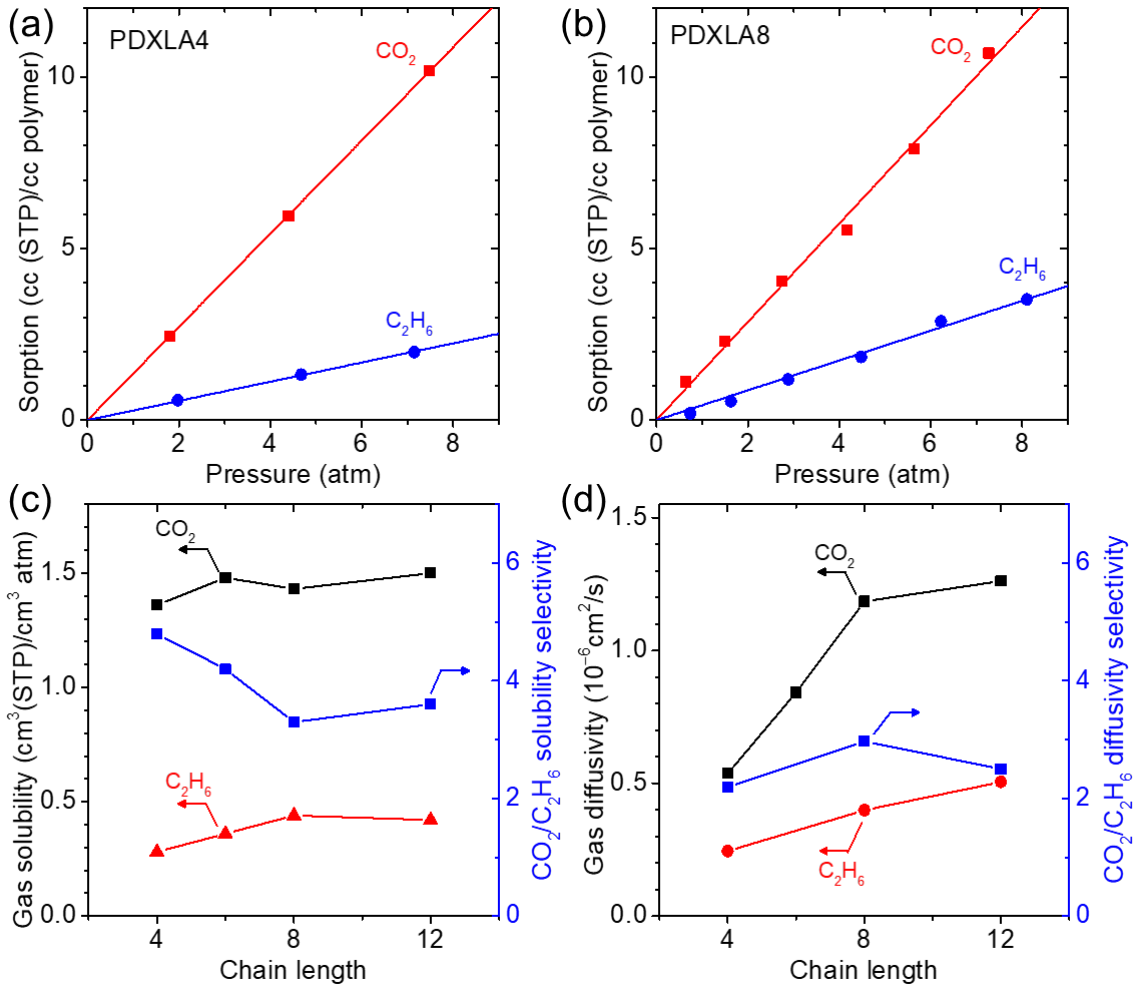

Figure 4. Gas sorption isotherms of (a) PDXLA4 and (b) PDXLA8 at 35 °C. The lines are the best fits of Henry's law. Effect of the DXL chain length on (c) gas solubility and CO_2/C_2H_6 solubility selectivity and (d) gas diffusivity and CO_2/C_2H_6 diffusivity selectivity.

As gas solubility is independent of the *n* values in PDXLAn, the increase of gas permeability with increasing *n* value can be ascribed to the increase in gas diffusivity. Figure 4d confirms that both CO_2 and C_2H_6 diffusivity increase significantly with increasing DXL chain length because of the increased *FFV* and lowered T_g. For example, CO_2 diffusivity increases from 5.4×10^{-7} cm^2/s for PDXL4 to 1.2×10^{-6} cm^2/s for PDXL8 by 120%. Figure 4d presents that CO_2

has much higher diffusivity than C_2H_6 because of the smaller kinetic diameter for CO_2, and the CO_2/C_2H_6 diffusivity selectivity is 2 – 3, comparable with that of PEGA7 (cf. Table S2).

Potential of PDXLA8 for mixed-gas CO_2/N_2 separation. PDXLA8 exhibits both good mechanical properties and CO_2/N_2 separation performance at 35 °C, and thus, it was thoroughly tested with CO_2/N_2 mixtures at various temperatures (Table S3). When tested with a mixed gas (CO_2:N_2=15:85) at 6.2 bar and 35 °C, the sample shows CO_2 permeability of 190 ± 4 Barrer, N_2 permeability is 3.3 ± 0.2 Barrer, and CO_2/N_2 selectivity of 57 ± 3 (cf. Figure 5a). By contrast, the polymer exhibits pure-gas permeability of 240 Barrer for CO_2 and 3.9 Barrer for N_2 at 6.2 bar and 35 °C (cf. Table S3). This difference between pure- and mixed-gas permeability is often attributed to the opposite effects of gas compression (decreasing *FFV*) and CO_2 plasticization (enhancing polymer chain flexibility).[28, 41, 42] The presence of non-plasticizing N_2 in the gas mixture compresses the sample and mitigates the CO_2 plasticization, reducing CO_2 permeability, while the existence of CO_2 neutralizes the compression and maintains N_2 permeability.

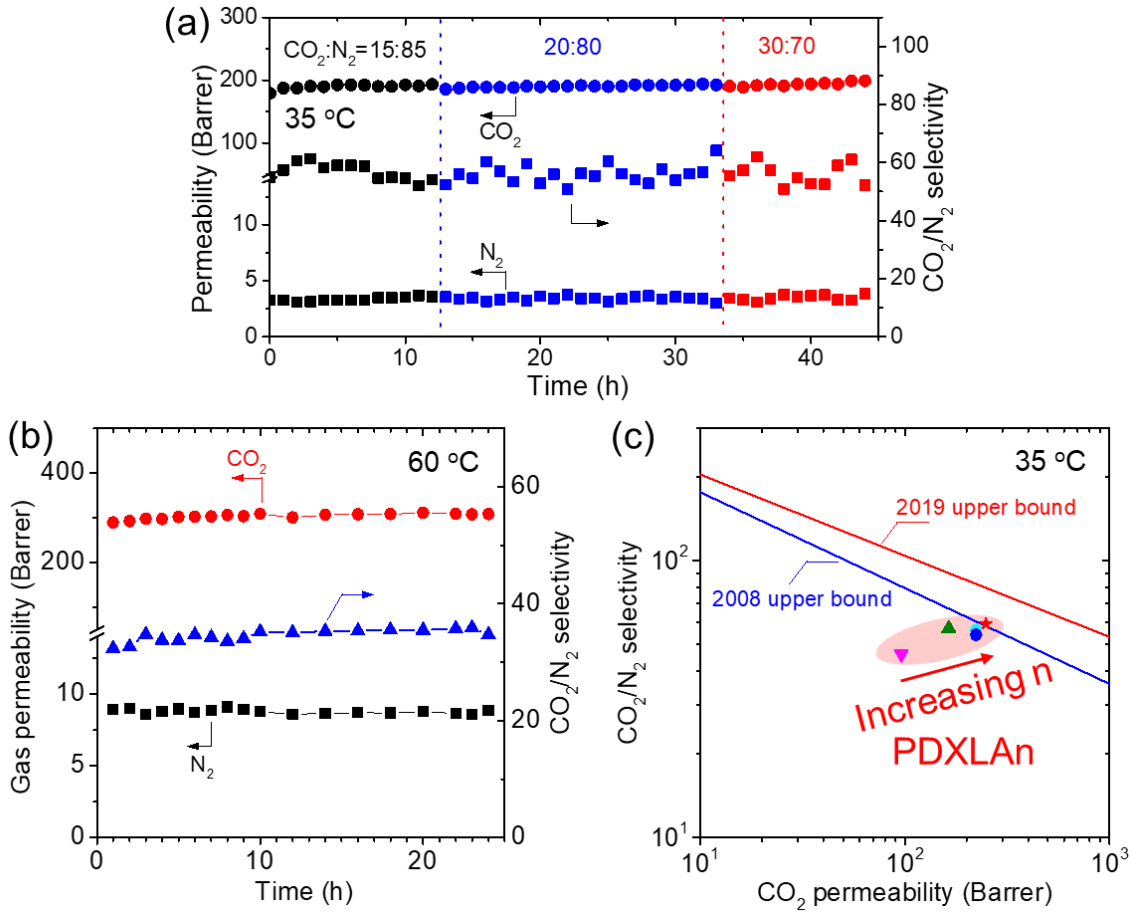

Figure 5. Mixed-gas CO_2/N_2 separation performance of PDXLA8. (a) Effect of the feed gas composition on the separation performance at 11.9 bar and 35 °C. (b) CO_2/N_2 separation performance at 11.9 bar and 60 °C for the CO_2/N_2 mixture (20/80). (c) Comparison with the 2008[43] and 2019[44] Roberson upper bounds at 35 °C.

Figure 5a also illustrates the effect of feed gas composition on the separation performance of PDXLA8. Increasing the CO_2 concentration from 15% to 30% has a negligible effect on CO_2 permeability and CO_2/N_2 selectivity. Additionally, PDXLA8 displays stable separation performance during the 45-h continuous test.

Figure 5b presents the mixed-gas CO_2/N_2 separation performance of PDXLA8 at 60 °C, a typical temperature for the flue gas from coal-fired power plants.[3] Increasing the temperature from 35 to 60 °C increases the mixed-gas CO_2 permeability from 190 to 300 Barrer and N_2 permeability from 3.3 to 8.7 Barrer and decreases CO_2/N_2 selectivity from 56 to 35. Moreover, PDXLA8 shows stable separation performance at 60 °C for a continuous test of 30 h, indicating its good thermal stability.

Figure 5c demonstrates the excellent CO_2/N_2 separation performance of the PDXLAn in Robeson's upper bound plot.[32, 43] Membrane materials exhibiting higher permeability often show lower selectivity. PDXLA8 exhibits CO_2/N_2 separation properties near the 2008 upper bound and below 2019 upper bound (which is defined by PIMs[44] and MMMs[45]). Together with its good stability at high temperatures, PDXLA8 is promising for industrial applications. Although some facilitated transport membranes, such as polyvinyl amine (PVAm), show CO_2/N_2 separation performance above 2019 upper bound,[1] their performance is highly dependent on the water content. In practical applications, the water vapor contents in the feed and permeate need to be carefully controlled to retain the excellent CO_2/N_2 separation performance, which increases the complexity of the membrane system.

Potential of PDXLA8 for mixed-gas CO_2/CH_4 separation. PDXLA8 was also investigated for CO_2/CH_4 separation at various feed pressures, feed gas compositions, and temperatures due to its balanced CO_2 permeability and CO_2/CH_4 selectivity. Figure 6a shows that both CO_2 and CH_4 permeability increase slightly with increasing CO_2 partial pressure at 35 °C and 6.5 bar because of the plasticization effect. For example, CO_2 permeability increases from 186 ± 3 (10% CO_2 in the feed gas) to 204 ± 3 Barrer (80% CO_2 in the feed gas). Similar to the mixed-gas CO_2/N_2 tests, the mixed-gas CO_2 permeability is lower than the pure-gas values due to the

compression by less condensable CH_4. In addition, the plasticization decreases the CO_2/CH_4 selectivity from 14 ± 1 (10% CO_2 in the feed gas) to 12 ± 1 (80% CO_2 in the feed gas), which is a typical phenomenon observed in polymers.[46, 47]

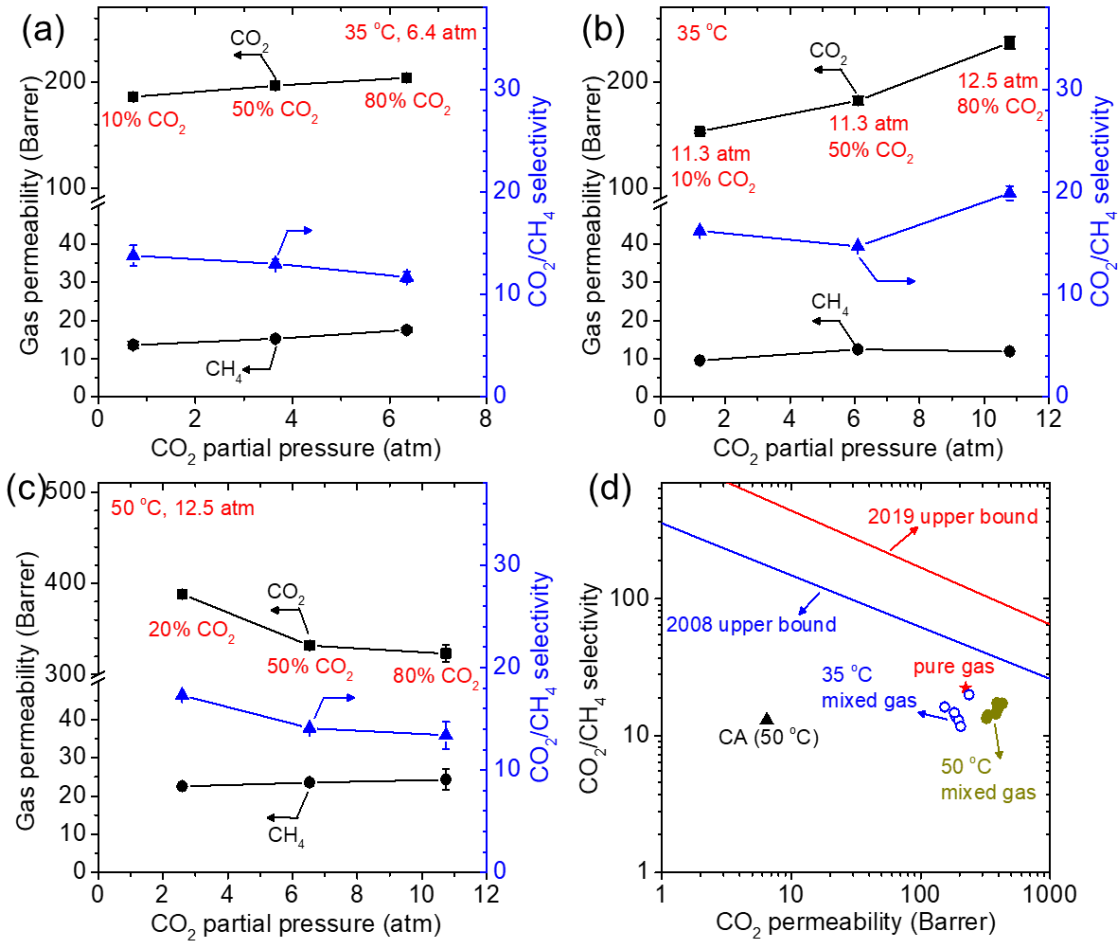

Figure 6. Influence of CO_2 partial pressure on the mixed-gas CO_2/CH_4 separation performance of PDXLA8 at (a, b) 35 °C and (c) 50 °C. (d) Comparison with CA in the 2008[43] and 2019[44] Roberson upper bounds at 35 °C for CO_2/CH_4 separation.

Figure 6a,b shows that increasing the total feed pressure increases CO_2/CH_4 selectivity at 35 °C. For example, increasing the feed pressure from 6.5 to 11.4 bar for the CO_2:CH_4 mixture (10:90) decreases CO_2 permeability from 190 to 150 Barrer and increases CO_2/CH_4 selectivity

from 14 ± 1 to 16 ± 1 because of the compaction at high pressures. By contrast, increasing the feed pressure from 7.1 to 12.7 bar for CO_2:CH_4 (80:20) increases CO_2 permeability from 200 to 240 Barrer and decreases the CH_4 permeability from 18 to 12 Barrer because of the competitive effect of plasticization caused by CO_2 sorption and the compaction induced by high pressure. Consequently, the CO_2/CH_4 selectivity improves from 12 to 20.

Figure 6c shows that increasing the temperature enhances gas permeability and reduces CO_2/CH_4 selectivity. For example, increasing the temperature from 35 to 50 °C increases CO_2 permeability from 240 to 320 Barrer and decreases CO_2/CH_4 selectivity from 20 to 13 when tested with CO_2:CH_4 (80:20) at 12.7 bar. Interestingly, different from the CO_2 plasticization effect observed at 35 °C, increasing the CO_2 partial pressure at 50 °C decreases CO_2 permeability and CO_2/CH_4 selectivity. Figure 6d compares PDXLA8 with cellulose acetates (CA), the membrane material used in industrial CO_2/CH_4 separation, in the 2008 and 2019 Roberson upper bounds. PDXLA8 exhibits CO_2/CH_4 selectivity similar to and CO_2 permeability much higher than CA (indicating its potential for industrial applications), though its separation performance is below the upper bound. However, PDXLA8 exhibits higher permeability of C2+ hydrocarbons (C_2H_4, C_2H_6, C_3H_6, and C_3H_8) than CH_4 (Table S4) and thus much lower selectivity of CO_2/C2+ hydrocarbons than CA, leading to higher hydrocarbon loss.[47] Nevertheless, biogas and landfill gas contain mainly CH_4 and CO_2, and PDXLA8 does not suffer from the disadvantage of the high loss of C2+ hydrocarbons.

Figure 7 demonstrates the stability of PDXLA8 at different feed gas conditions and temperatures. PDXLA8 displays stable CO_2 permeability and CO_2/CH_4 selectivity for ~100 h at 35 °C (Figure 7a) and 50 °C (Figure 7b).

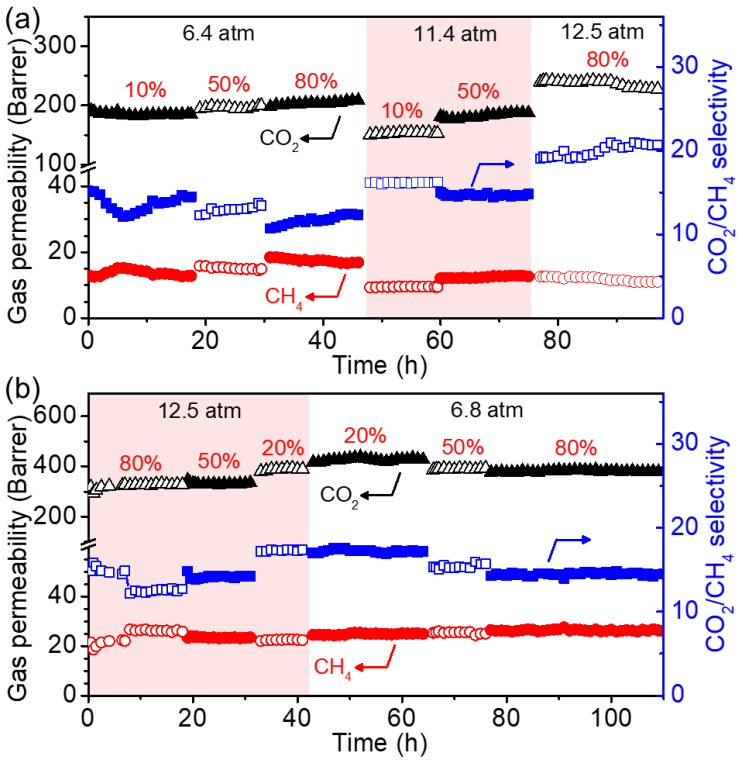

Figure 7. Stability of PDXLA8 during the mixed-gas CO_2/CH_4 separation tests at (a) 35 °C and (b) 50 °C at feed pressures ranging from 6.5 to 12.7 bar and CO_2 feed concentration varying from 10% to 80%.

■ CONCLUSIONS

A systematic series of hyperbranched PDXLAn with *n* values ranging from 4 to 12 were synthesized using a well-controlled method and thoroughly examined for membrane CO_2/N_2 and CO_2/CH_4 separation. Increasing *n* value decreases T_g and increases *FFV* because of the decreased content of –OH groups, improving gas diffusivity and permeability. Increasing *n* value enhances CO_2/C_2H_6 solubility selectivity due to the increased content of the CO_2-philic ether oxygen groups. By contrast, the *n* value has essentially no effect on CO_2 solubility because of the decreased *FFV*. When tested with model flue gas containing 20% CO_2 and 80% N_2, PDXLA8 demonstrates robust

CO_2/N_2 separation performance at temperatures up to 60 °C, superior to 2008 upper bound. PDXLA8 also shows mixed-gas CO_2/CH_4 separation performance superior to CA, a workhorse material for industrial gas separation. This work demonstrates that hyperbranched architectures are an effective tool to design amorphous polymers incorporating high content of highly polar groups with a great tendency to crystallize and that chain end groups have an important impact on structures and gas transport properties.

■ MATERIALS AND METHODS

Materials. Anhydrous DXL (99.8%), triethylamine (TEA, ≥99%), and HCPK (99%) were obtained from Sigma-Aldrich Corporation (St. Louis, MO). 2-Hydroxyethyl acrylate (HEA, 97%) and triflic acid (TfOH, 99%) were acquired from Acros Organics (Fair Lawn, NJ). Dichloromethane (DCM, ≥99.5%) was procured from Fisher Scientific (Hampton, NH) and dried with 3A molecular sieves (Acros Organics) before use. CO_2, H_2, and N_2 (99.9%) were supplied by Airgas, Inc. (Radnor, PA).

Synthesis of PDXLAn. DXLAn was first synthesized following our previous work with minor modifications,[31, 32] and the chain length (*n* value) of DXLAn is almost the same as the molar ratio of DXL to HEA. As an example of synthesizing DXLA8, a flask was first purged with argon for 10 min to remove O_2 and H_2O and then kept in an ice bath. Second, DCM (50 mL), HEA (7.34 mL, 62 mmol), and TfOH (0.607 mL, 6.89 mmol) were added into the flask, and the solution was stirred at 600 rpm for 10 min. Third, DXL (35 ml, 500 mmol) was added slowly to the solution using a syringe under a continuous argon purge. After 10 min, the flask was transferred to a water bath (21 °C) for the reaction to continue for 3 h. Fourth, TEA (2.5 mL) was added to terminate the reaction, and the solution was stirred for another 10 min. Finally, the solution was extracted with

100 mL deionized (DI) water 3 times, and the DCM phase was rotary-evaporated under vacuum at 50 ℃ for 3 h to obtain the DXLAn product. The yield of DXLAn is about 75% (based on the mass of the added DXL and HEA).

To synthesize PDXLAn, the prepolymer solution was prepared by mixing DXLAn (3.0 g) and HCPK (3.0 mg).[28, 32] The solution was photopolymerized using 254-nm UV light at 3.0 mW cm^{-2} for 5 min. The film thickness (~200 μm) was measured using Starrett 2900 micrometer (The L.S. Starrett Co., MA). All the PDXLAn films were used for gas permeation tests without further treatment.

Characterizations. Rigaku Ultima IV diffractometer with Cu Kα radiation (Rigaku, JP) was used to obtain X-ray diffraction patterns. ATR-FTIR spectra were collected using a vertex 70 Burker spectrometer (Billerica, MA). NMR spectra were recorded on a Varian Inova-500 spectrometer. Mass spectra were obtained using a Fourier Transform Ion Cyclotron Resonance Mass Spectrometer (FT-ICR MS) (Solarix 12 T, Bruker) using electrospray ionization (ESI). Thermal transitions of the polymers were determined using Q2000 DSC (TA Instruments, New Castle, DE). Samples were scanned from -90 ℃ to 80 ℃ in N_2 atmosphere at 10 ℃ min^{-1} for three cycles, and the last heating cycle was used to obtain the properties. The mechanical properties of PDXLAn films were determined using static tensile loading with a dynamic mechanical analysis (DMA, Q800 TA Instrument). The tensile tests were conducted at temperatures of 25°C. Uniaxial tensile loading on the sample stripes (20 mm × 3-4 mm) was carried out with an initial strain of 0.01% at a constant strain rate of 1.0%/min until the sample fractured. The film density was measured using Mettler Toledo XS64 with a density measurement kit based on Archimedes' principle.[28]

Pure-gas permeability (P_A, Barrer) was determined using a constant-volume and variable-pressure system at 35 °C.[48] The leak rate of the system was measured before permeation tests and should be ten times lower than the steady-state gas permeation rate. Mixed-gas CO_2 and N_2 permeability were measured by a constant-pressure and variable-volume system with H_2 as a sweep gas on the permeate side.[32, 48] The gas permeability has an uncertainty of ≈10% estimated using an error propagation analysis unless specified.[49]

A dual-volume and dual-transducer system was used to determine gas sorption isotherms at 35 °C.[50] Gas solubility (S_A, cm^3 (STP) cm^{-3} atm^{-1}) can be calculated using Equation 3:

$$S_A = C_A/p_A \tag{3}$$

where C_A is the gas sorption (cm^3 (STP) cm^{-3}), and p_A is the gas pressure at equilibrium (atm). The solubility has an uncertainty of <10% using the error propagation analysis.[49] Based on the solution and diffusion mechanism, gas diffusivity (D_A, cm^2 s^{-1}) can be obtained using Equation 4:

$$D_A = P_A/S_A \tag{4}$$

■ ASSOCIATED CONTENT

Supporting Information

The Supporting Information is available free of charge at https://pubs.acs.org.

Figure S1-S3: NMR, MS, and FT-IR spectra of DXLn and PDXLAn films.

Figure S4-S6: XRD, density, mechanical properties, and gas sorption of PDXLAn films.

Table S1-S4: Physical properties and separation performance of PDXLAn films.

■ AUTHOR INFORMATION

Corresponding Author

*E-mail: haiqingl@buffalo.edu

Author Contributions

All authors contributed to the scientific discussion and manuscript preparation. H.L. and L.H. conceived the approach and conducted experimental designs. L.H., W.G., H.M., S.S., and T.T. fabricated and characterized materials. L.H. wrote the first draft of the manuscript, and all authors contributed to manuscript editing. H.L. supervised the project.

Notes

The authors declare no competing financial interest.

■ ACKNOWLEDGMENT

This work received financial support from the U.S. Department of Energy National Energy Technology Laboratory (DE-FE0031736), the New York State Foundation for Science, Technology and Innovation (NYSTAR), and the U.S. National Science Foundation (1554236).

■ REFERENCES

(1) Han, Y.; Ho, W. S., Polymeric membranes for CO_2 separation and capture, *J. Membr. Sci.* **2021,** *628*, 119244, DOI 10.1016/j.memsci.2021.119244.

(2) Park, H.; Kamcev, J.; Robeson, L. M.; Elimelech, M.; Freeman, B. D., Maximizing the right stuff: The trade-off between membrane permeability and selectivity, *Science* **2017,** *356* (6343), eaab0530, DOI 10.1126/science.aab0530.

(3) Merkel, T. C.; Lin, H.; Wei, X.; Baker, R. W., Power plant post-combustion carbon dioxide capture: An opportunity for membranes, *J. Membr. Sci.* **2010,** *359* (1-2), 126-139, DOI 10.1016/j.memsci.2009.10.041.

(4) Luo, S.; Zhang, Q.; Zhu, L.; Lin, H.; Kazanowska, B. A.; Doherty, C. M.; Hill, A. J.; Gao, P.; Guo, R., Highly Selective and Permeable Microporous Polymer Membranes for Hydrogen Purification and CO_2 Removal from Natural Gas, *Chem. Mater.* **2018,** *30* (15), 5322-5332, DOI 10.1021/acs.chemmater.8b02102.

(5) Lee, J.; Kim, J.; Kim, J.; Jo, H.; Park, H.; Seong, J.; Lee, Y., Densification-induced hollow fiber membranes using crosslinked thermally rearranged (XTR) polymer for CO_2 capture, *J. Membr. Sci.* **2019,** *573*, 393-402, DOI 10.1016/j.memsci.2018.12.023.

(6) Park, H.; Jung, C.; Lee, Y.; Hill, A. J.; Pas, J. P.; Mudie, S. T.; Van Wagner, E.; Freeman, B. D.; Cookson, D. J., Polymers with Cavities Tuned for Fast Selective Transport of Small Molecules and Ions, *Science* **2007,** *318*, 254-258, DOI 10.1126/science.1146744.

(7) Du, N.; Park, H.; Robertson, G. P.; Dal-Cin, M. M.; Visser, T.; Scoles, L.; Guiver, M. D., Polymer nanosieve membranes for CO_2-capture applications, *Nat. Mater.* **2011,** *10* (5), 372-375, DOI 10.1038/nmat2989.

(8) Carta, M.; Malpass-Evans, R.; Croad, M.; Rogan, Y.; Jansen, J. C.; Bernardo, P.; Bazzarelli, F.; McKeown, N. B., An efficient polymer molecular sieve for membrane gas separations, *Science* **2013,** *339* (6117), 303-307, DOI 10.1126/science.1228032.

(9) Qiao, Z.; Zhao, S.; Sheng, M.; Wang, J.; Wang, S.; Wang, Z.; Zhong, C.; Guiver, M. D., Metal-induced ordered microporous polymers for fabricating large-area gas separation membranes, *Nat. Mater.* **2019,** *18*, 163-168, DOI 10.1038/s41563-018-0221-3.

(10) Deng, X.; Zou, C.; Han, Y.; Lin, L.; Ho, W. S. W., Computational Evaluation of Carriers in Facilitated Transport Membranes for Postcombustion Carbon Capture, *J. Phys. Chem. C* **2020,** *124* (46), 25322-25330, DOI 10.1021/acs.jpcc.0c07627.

(11) Liu, L.; Sanders, E. S.; Kulkarni, S. S.; Hasse, D. J.; Koros, W. J., Sub-ambient temperature flue gas carbon dioxide capture via Matrimid (R) hollow fiber membranes, *J. Membr. Sci.* **2014,** *465*, 49-55, DOI 10.1016/j.memsci.2014.03.060.

(12) Deng, J.; Dai, Z.; Hou, J.; Deng, L., Morphologically Tunable MOF Nanosheets in Mixed Matrix Membranes for CO_2 Separation, *Chem. Mater.* **2020,** *32* (10), 4174-4184, DOI 10.1021/acs.chemmater.0c00020.

(13) Zhu, B.; Jiang, X.; He, S.; Yang, X.; Long, J.; Zhang, Y.; Shao, L., Rational design of poly(ethylene oxide) based membranes for sustainable CO_2 capture, *J. Mater. Chem. A* **2020,** *8*, 24233-24252, DOI 10.1039/D0TA08806D.

(14) Lin, H.; Freeman, B. D., Materials selection guidelines for membranes that remove CO_2 from gas mixtures, *J. Mol. Struct.* **2005,** *739* (1-3), 57-74, DOI 10.1016/j.molstruc.2004.07.045.

(15) Lin, H.; Van Wagner, E.; Freeman, B. D.; Toy, L. G.; Gupta, R. P., Plasticization-enhanced hydrogen purification using polymeric membranes, *Science* **2006,** *311* (5761), 639-642, DOI 10.1126/science.1118079.

(16) Liu, J.; Hou, X.; Park, H.; Lin, H., High-performance polymers for membrane CO_2/N_2 separation, *Chem. Eur. J.* **2016,** *22* (45), 15980-15990, DOI 10.1002/chem.201603002.

(17) Bondar, V. I.; Freeman, B. D.; Pinnau, I., Gas sorption and characterization of poly(ether-b-amide) segmented block copolymers, *J. Polym. Sci., Part B: Polym. Phys.* **1999,** *37* (17), 2463-2475, DOI 10.1002/(Sici)1099-0488(19990901)37:17<2463::Aid-Polb18>3.0.Co;2-H.

(18) Kim, J.; Ha, S.; Lee, Y., Gas permeation of poly(amide-6-b-ethylene oxide) copolymer, *J. Membr. Sci.* **2001,** *190* (2), 179-193, DOI 10.1016/S0376-7388(01)00444-6.

(19) Meshkat, S.; Kaliaguine, S.; Rodrigue, D., Enhancing CO_2 separation performance of Pebax® MH-1657 with aromatic carboxylic acids, *Sep. Purif. Technol.* **2019,** *212*, 901-912, DOI 10.1016/j.seppur.2018.12.008.

(20) Car, A.; Stropnik, C.; Yave, W.; Peinemann, K. V., Tailor-made polymeric membranes based on segmented block copolymers for CO_2 separation, *Adv. Funct. Mater.* **2008,** *18* (18), 2815-2823, DOI 10.1002/adfm.200800436.

(21) Yave, W.; Szymczyk, A.; Yave, N.; Roslaniec, Z., Design, synthesis, characterization and optimization of PTT-b-PEO copolymers: A new membrane material for CO_2 separation, *J. Membr. Sci.* **2010,** *362* (1-2), 407-416, DOI 10.1016/j.memsci.2010.06.060.

(22) Reijerkerk, S. R.; Wessling, M.; Nijmeijer, K., Pushing the limits of block copolymer membranes for CO_2 separation, *J. Membr. Sci.* **2011,** *378* (1), 479-484, DOI 10.1016/j.memsci.2011.05.039.

(23) Rodriguez, C. G.; Chwatko, M.; Park, J.; Bentley, C. L.; Freeman, B. D.; Lynd, N. A., Compositionally controlled polyether membranes via mono(mu-alkoxo)bis(alkylaluminum)-Initiated chain-growth network epoxide polymerization: synthesis and transport properties, *Macromolecules* **2020,** *53* (4), 1191-1198, DOI 10.1021/acs.macromol.9b02318.

(24) Kusuma, V. A.; Freeman, B. D.; Borns, M. A.; Kalika, D. S., Influence of chemical structure of short chain pendant groups on gas transport properties of cross-linked poly(ethylene oxide) copolymers, *J. Membr. Sci.* **2009,** *327* (1-2), 195-207, DOI 10.1016/j.memsci.2008.11.022.

(25) Lin, H.; Wagner, E.; Swinnea, J.; Freeman, B.; Pas, S.; Hill, A.; Kalakkunnath, S.; Kalika, D., Transport and structural characteristics of crosslinked poly(ethylene oxide) rubbers, *J. Membr. Sci.* **2006,** *276* (1-2), 145-161, DOI 10.1016/j.memsci.2005.09.040.

(26) Hirayama, Y.; Kase, Y.; Tanihara, N.; Sumiyama, Y.; Kusuki, Y.; Haraya, K., Permeation properties to CO_2 and N_2 of poly(ethylene oxide)-containing and crosslinked polymer films, *J. Membr. Sci.* **1999,** *160* (1), 87-99, DOI 10.1016/S0376-7388(99)00080-0.

(27) Liu, J.; Fulong, C. R. P.; Hu, L.; Huang, L.; Zhang, G.; Cook, T. R.; Lin, H., Interpenetrating networks of mixed matrix materials comprising metal-organic polyhedra for membrane CO_2 capture, *J. Membr. Sci.* **2020,** *606*, 118122, DOI 10.1016/j.memsci.2020.118122.

(28) Huang, L.; Liu, J.; Lin, H., Thermally stable, homogeneous blends of cross-linked poly(ethylene oxide) and crown ethers with enhanced CO_2 permeability, *J. Membr. Sci.* **2020,** *610*, 118253, DOI 10.1016/j.memsci.2020.118253.

(29) Hu, L.; Liu, J.; Zhu, L.; Hou, X.; Huang, L.; Lin, H.; Cheng, J., Highly permeable mixed matrix materials comprising ZIF-8 nanoparticles in rubbery amorphous poly(ethylene oxide) for CO_2 capture, *Sep. Purif. Technol.* **2018,** *205*, 58-65, DOI 10.1016/j.seppur.2018.05.012.

(30) Jiang, X.; Li, S.; Shao, L., Pushing CO_2-philic membrane performance to the limit by designing semi-interpenetrating networks (SIPN) for sustainable CO_2 separations, *Energy Environ. Sci.* **2017,** *10* (6), 1339-1344, DOI 10.1039/c6ee03566c.

(31) Liu, J.; Zhang, G.; Clark, K.; Lin, H., Maximizing ether oxygen content in polymers for membrane CO_2 removal from natural gas, *ACS Appl. Mater. Interfaces* **2019,** *11* (11), 10933-10940, DOI 10.1021/acsami.9b01079.

(32) Liu, J.; Zhang, S.; Jiang, D.; Doherty, C. M.; Hill, A. J.; Cheng, C.; Park, H. B.; Lin, H., Highly polar but amorphous polymers with robust membrane CO_2/N_2 separation performance, *Joule* **2019,** *3* (8), 1881-1894, DOI 10.1016/j.joule.2019.07.003.

(33) Franta, E.; Kubisa, P.; Kada, S. O.; Reibel, L., Synthesis of functionalized poly(1,3-dioxolane), *Makromol. Chem. Macromol. Symp.* **1992,** *60* (1), 145-154, DOI 10.1002/masy.19920600113.
(34) Franta, E.; Lutz, P.; Reibel, L.; Sahli, N.; Kada, S. O.; Belbachir, M., Functionalization of poly(1,3-dioxolane), *Macromol. Symp.* **1994,** *85* (1), 167-174, DOI 10.1002/masy.19940850112.
(35) Feldstein, M. M.; Shandryuk, G. A.; Platé, N. A., Relation of glass transition temperature to the hydrogen-bonding degree and energy in poly(N-vinyl pyrrolidone) blends with hydroxyl-containing plasticizers. Part 1. Effects of hydroxyl group number in plasticizer molecule, *Polymer* **2001,** *42* (3), 971-979, DOI 10.1016/S0032-3861(00)00445-6.
(36) van der Sman, R. G. M., Predictions of glass transition temperature for hydrogen bonding biomaterials, *J. Phys. Chem. B* **2013,** *117* (50), 16303-16313, DOI 10.1021/jp408184u.
(37) Lin, H.; Freeman, B. D.; Kalakkunnath, S.; Kalika, D. S., Effect of copolymer composition, temperature, and carbon dioxide fugacity on pure- and mixed-gas permeability in poly(ethylene glycol)-based materials: Free volume interpretation, *J. Membr. Sci.* **2007,** *291* (1-2), 131-139, DOI 10.1016/j.memsci.2007.01.001.
(38) Lin, H.; Freeman, B. D., Gas permeation and diffusion in cross-linked poly(ethylene glycol diacrylate), *Macromolecules* **2006,** *39* (10), 3568-3580, DOI 10.1021/ma051686o.
(39) Lin, H.; Freeman, B. D., Gas solubility, diffusivity and permeability in poly(ethylene oxide), *J. Membr. Sci.* **2004,** *239* (1), 105-117, DOI 10.1016/j.memsci.2003.08.031.
(40) Kelman, S.; Lin, H.; Sanders, E. S.; Freeman, B. D., CO_2/C_2H_6 separation using solubility selective membranes, *J. Membr. Sci.* **2007,** *305*, 57-68, DOI 10.1016/j.memsci.2007.07.035.
(41) Merkel, T. C.; Bondar, V. I.; Nagai, K.; Freeman, B. D.; Pinnau, I., Gas sorption, diffusion, and permeation in poly(dimethylsiloxane), *J. Polym. Sci., Part B: Polym. Phys.* **2000,** *38* (3), 415-434, DOI 10.1002/(sici)1099-0488(20000201)38:3<415::Aid-polb8>3.0.Co;2-z.
(42) Wu, F.; Li, L.; Xu, Z.; Tan, S.; Zhang, Z., Transport study of pure and mixed gases through PDMS membrane, *Chem. Eng. J.* **2006,** *117* (1), 51-59, DOI 10.1016/j.cej.2005.12.010.
(43) Robeson, L. M., The upper bound revisited, *J. Membr. Sci.* **2008,** *320* (1-2), 390-400, DOI 10.1016/j.memsci.2008.04.030.
(44) Comesaña-Gándara, B.; Chen, J.; Bezzu, C. G.; Carta, M.; Rose, I.; Ferrari, M.-C.; Esposito, E.; Fuoco, A.; Jansen, J. C.; McKeown, N. B., Redefining the Robeson upper bounds for CO_2/CH_4 and CO_2/N_2 separations using a series of ultrapermeable benzotriptycene-based polymers of intrinsic microporosity, *Energy Environ. Sci.* **2019,** *12* (9), 2733-2740, DOI 10.1039/c9ee01384a.
(45) Ashtiani, S.; Sofer, Z.; Průša, F.; Friess, K., Molecular-level fabrication of highly selective composite ZIF-8-CNT-PDMS membranes for effective CO_2/N_2, CO_2/H_2 and olefin/paraffin separations, *Sep. Purif. Techn.* **2021,** *274*, 119003, DOI 10.1016/j.seppur.2021.119003.
(46) Bos, A.; Pünt, I. G. M.; Wessling, M.; Strathmann, H., CO_2-induced plasticization phenomena in glassy polymers, *J. Membr. Sci.* **1999,** *155* (1), 67-78, DOI 10.1016/S0376-7388(98)00299-3.
(47) Lin, H.; Van Wagner, E.; Raharjo, R.; Freeman, B. D.; Roman, I., High performance polymer membranes for natural gas sweetening, *Adv. Mater.* **2006,** *18* (18), 39-44, DOI 10.1002/adma.200501409.

(48) Zhu, L.; Swihart, M. T.; Lin, H., Tightening polybenzimidazole (PBI) nanostructure via chemical cross-linking for membrane H_2/CO_2 separation, *J. Mater. Chem. A* **2017,** *5* (37), 19914-19923, DOI 10.1039/c7ta03874g.
(49) Bevington, P. R.; Robinson, D. K., *Data Reduction and Error Analysis for the Physical Sciences*. 2nd ed.; McGraw-Hill, Inc.: New York, 1992.
(50) Yavari, M.; Fang, M.; Nguyen, H.; Merkel, T. C.; Lin, H.; Okamoto, Y., Dioxolane-based perfluoropolymers with superior membrane gas separation properties, *Macromolecules* **2018,** *51* (7), 2489-2497, DOI 10.1021/acs.macromol.8b00273.